

Resonance Modes of Interstitial Atoms in fcc Metals

P. H. Dederichs and C. Lehmann

Institut für Festkörperforschung, Kernforschungsanlage Jülich, Jülich, W. Germany

and

A. Scholz

Zentralinstitut für Angewandte Mathematik, Kernforschungsanlage Jülich, Jülich, W. Germany

(Received 17 September)

By means of computer simulation of a copper lattice, we have found two resonance modes of the (split) interstitial configuration. The low frequencies of about $\omega_{\max}/7$ are due to the strong negative "leaf springs" typical for the strongly compressed lattice around the interstitial atom. It seems very likely that many longstanding problems associated with point defects can be explained in terms of such modes.

The vibrations of an ideal lattice can be considerably changed by introducing point defects. The square of the characteristic frequency associated with the defect is $\omega^2 = f_d/m_d$, where f_d is a typical coupling constant and m_d the defect mass. Two kinds of new modes can occur: (i) localized modes with frequencies above the maximum frequency ω_{\max} of the ideal lattice, if $f_d \gtrsim f$ and/or $m_d \lesssim m$; and (ii) resonance modes with $\omega \ll \omega_{\max}$, if $f_d \ll f$ and/or $m_d \gg m$. In the case of a self-interstitial ($m_d = m$) in metals, the lattice is locally strongly compressed ($f_d \gg f$). Therefore this simple picture suggests that only localized modes, but no resonance modes, exist.

The complicated dynamics of a self-interstitial in Cu has been investigated by computer simulation, using a Born-Mayer potential as described earlier.¹ In this model the $\langle 100 \rangle$ -split interstitial (dumbbell) turns out to be the only stable defect configuration. This is further true for a Morse

potential which has also been used. (Experimentally, the dumbbell has been confirmed to be the interstitial configuration in Al.^{2,3}) By transferring small momenta to the dumbbell atoms, several localized modes have been found.^{1,4}

With the extension of these computer calculations, we have now found two unexpected resonance modes with frequencies of about $\omega_{\max}/7$. Figures 1 and 2 show the displacements of the dumbbell atoms and the nearest neighbors for these two modes. In the first mode (Fig. 1) the two dumbbell atoms move with equal amplitude along the dumbbell axis (symmetry A_{1u}), whereas the second mode (Fig. 2) is a libration of the dumbbell (symmetry E_g^1). Figure 3 shows as a typical result of the computer calculations the motion of a dumbbell atom in the libration mode, initiated by an impulse to the dumbbell atoms in opposite directions along the x axis at time $t=0$ (a total energy transfer of 0.03 eV). The displace-

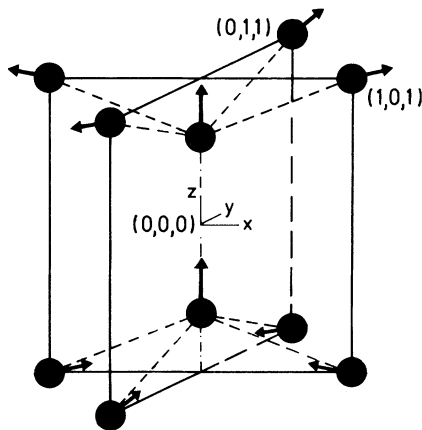


FIG. 1. Schematic representation of the axial resonant mode (symmetry A_{1u}) of the $\langle 100 \rangle$ -split interstitial in a fcc lattice.

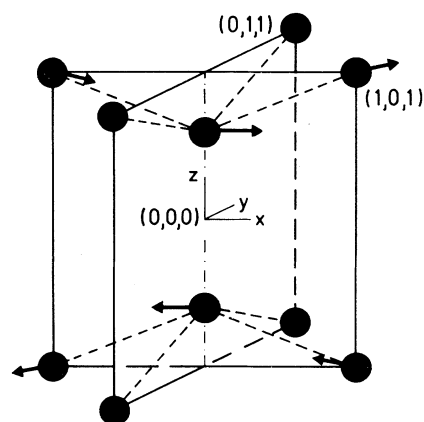


FIG. 2. Schematic representation of the libration resonant mode (symmetry E_g^1) of the $\langle 100 \rangle$ -split interstitial in a fcc lattice.

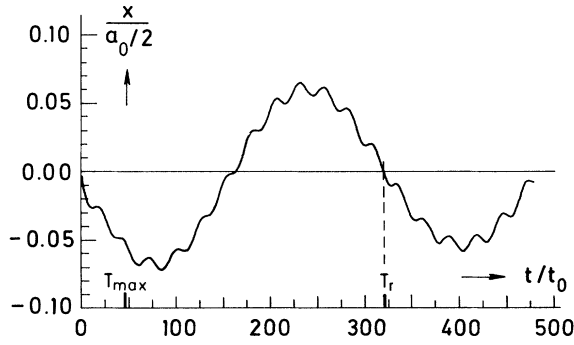


FIG. 3. Displacement of upper dumbbell atom in the libration mode versus time. T_r is the vibration time of the resonance mode; $T_{\max} = 2\pi/\omega_{\max}$; $a_0 = 3.61 \text{ \AA}$; $t_0 = 3.27 \times 10^{-15} \text{ sec}$; the Morse potential $V(R) = D\{\exp[-2\alpha \times (R - R_0)]\}$, with $D = 0.180 \text{ eV}$, $\alpha = 2.33 \text{ \AA}^{-1}$, $R_0 = 2.57 \text{ \AA}$.

ment of the dumbbell atom exhibits the low-frequency resonance mode which is only slightly damped, as is expected of a good resonance. Superimposed is a high-frequency and practically undamped localized mode which is also excited with this initial condition. The other, axial, mode shows the same characteristics. For either potential, both modes are clearly resonant with frequencies differing by only about 30%.

The low frequencies of the resonance modes can be explained by the coupling constants for a central potential $V(R)$:

$$\varphi_{ij}(\vec{R}) = \partial_{x_i} \partial_{x_j} V(R) = \begin{pmatrix} f_{\parallel} & 0 & 0 \\ 0 & f_{\perp} & 0 \\ 0 & 0 & f_{\perp} \end{pmatrix},$$

where $f_{\parallel} = V''(R)$, $f_{\perp} = V'(R)/R$, and where the X_{\perp} axis coincides with the direction of the vector \vec{R} connecting the two atoms. The constant f_{\parallel} enters for displacements parallel to \vec{R} ("spiral spring"), whereas f_{\perp} enters for displacements perpendicular to \vec{R} ("leaf spring"). For an ideal lattice, $f_{\parallel} = f_{\parallel}^0$ is the dominating force constant and $f_{\perp} = f_{\perp}^0$ can be neglected in a first approximation. However, in the compressed region of an interstitial both force constants are much larger and f_{\perp} cannot be neglected. For the Born-Mayer potential one obtains for the interaction of the two dumbbell atoms $f_{\parallel} = 6.7f_{\parallel}^0$ and $f_{\perp} = -0.61f_{\parallel}^0$; and for the interaction between one dumbbell atom and its nearest neighbors, $f_{\parallel} = 4.0f_{\parallel}^0$ and $f_{\perp} = -0.35f_{\parallel}^0$. Thus, because of the strong repulsion of the atoms, f_{\perp} is always negative and becomes comparable to f_{\parallel}^0 . Two kinds of characteristic modes are possible: (1) vibrations which considerably stress the strong spiral springs in the interstitial

region, giving rise to high-frequency localized modes for which the relatively weak leaf springs are not important, and (2) vibrations which stress the strong spiral springs only slightly. In the latter case the negative leaf springs become important. They lower the frequency and hence give rise to resonance modes. We have also estimated the resonance frequencies analytically and found reasonable agreement with the computer results.

Such resonance modes should also occur for other interstitial structures (and also in other types of lattices), since, as a consequence of the strong interaction, the leaf springs in the interstitial region should always be comparable to f_{\parallel}^0 . These negative springs may even lower the resonance frequency for a particular position so much that eventually $\omega^2 < 0$. Then this interstitial position would be unstable. Thus the negative leaf springs introduce a tendency towards instability: They determine the stability or instability of a certain configuration and lead to resonance modes for the stable configurations.

The resonance modes seem to provide the general basis for the understanding of many poorly understood physical properties of the interstitial. Some important examples are briefly discussed for the case of a split interstitial:

(I) As has already been speculated by Flynn,⁵ low-frequency resonance modes could explain the diffusion of the interstitial at low temperatures.⁶ Indeed, if low-frequency modes are present, the thermal displacements are very large and may exceed a critical value when the modes get thermally populated. For example, the axial mode (Fig. 1) leads directly to a jump of the dumbbell into the adjacent position along the axis, whereas the libration mode (Fig. 2) leads to a rotation of the dumbbell by 90° . By combination of both modes the dumbbell jumps to the position of its nearest neighbor, rotating at the same time by 90° . This process has by far the lowest activation energy, in agreement with calculations by Johnson and Brown.⁷

(II) As a result of the low-frequency mode E_g^1 , the interstitial is strongly polarizable by an external shear stress. This explains the experimentally observed extreme softening of the lattice due to interstitials.⁸ Analytical calculations show⁹ that such modes always lead to large and negative changes of the elastic shear constants. The recently observed anisotropy of the shear modulus change in Al¹⁰ can be directly related to the symmetry of the dumbbell.

(III) Preliminary analytical calculations show

that the frequencies, and hence the stability, of a dumbbell depend very sensitively on the presence of a nearby vacancy. Thus the instability volume^{4,1} of a Frenkel pair and the correlated recovery stages⁶ should be closely related to resonance modes.

We gratefully acknowledge many fruitful discussions with G. Leibfried and W. Schilling. We also thank A. Goland for pointing out that our finding of the resonant modes is consistent with a reanalysis of earlier calculations by Gibson *et al.*⁴

¹A. Scholz and Chr. Lehmann, Phys. Rev. B 6, 813 (1972).

²P. Ehrhart and W. Schilling, Phys. Rev. D 8, 2604 (1973).

³G. Haubold and W. Schilling, private communication.
⁴J. B. Gibson, A. N. Goland, M. Milgram, and G. H. Vineyard, Phys. Rev. 120, 1229 (1960).

⁵C. P. Flynn, Phys. Rev. 171, 682 (1968).

⁶W. Schilling, G. Burger, K. Isebeck, and H. Wenzl, in *Vacancies and Interstitials in Metals*, edited by A. Seeger, D. Schuhmacher, W. Schilling, and J. Diehl (North-Holland, Amsterdam, 1970), p. 255.

⁷R. A. Johnson and E. Brown, Phys. Rev. 127, 446 (1962).

⁸H. Wenzl, in *Vacancies and Interstitials in Metals*, edited by A. Seeger, D. Schuhmacher, W. Schilling, and J. Diehl (North-Holland, Amsterdam, 1970), p. 363.

⁹P. H. Dederichs, to be published.

¹⁰K. H. Robrock and W. Schilling, private communication.

Compatibility Relationships for X-Ray Threshold Shapes

John D. Dow*

Department of Physics and Materials Research Laboratory, University of Illinois at Urbana-Champaign, Urbana, Illinois 61801

(Received 19 June 1973)

Bounds on the exponents of the many-electron x-ray threshold anomaly are obtained, and a relationship between soft- and hard-x-ray threshold shapes is derived. The spectra of Mg_xSb_{1-x} alloys and Al metal are shown to be inconsistent with the many-electron theory of threshold exponents.

Many-electron theories of the soft-x-ray absorption spectra of simple metals predict the "anomalous" absorption-threshold shape¹

$$\epsilon_2(\omega) \cong \sum_{i=0}^{\infty} A_i^2 \left(\frac{\hbar\omega - E_T}{\xi} \right)^{-\alpha_i} \theta(\hbar\omega - E_T). \quad (1)$$

A similar expression describes emission spectra. Here $\epsilon_2(\omega)$ is the imaginary part of the dielectric function, $\hbar\omega$ is the photon energy, E_T is the threshold energy, ξ is a parameter with dimensions of energy, $\theta(x)$ is the unit step function, $2\pi\hbar$ is Planck's constant, and A_i is proportional to the optical transition matrix element between a core electron initially localized at the origin and a spherical-wave conduction-band electron with angular momentum quantum number l . The exponents of the threshold law, α_i , can be expressed in terms of the partial-wave phase shifts δ_j for an electron at the Fermi energy experiencing the scattering potential of the hole²:

$$\alpha_i = 2 \frac{\delta_i}{\pi} - 2 \sum_{j=0}^{\infty} (2j+1) \left(\frac{\delta_j}{\pi} \right)^2. \quad (2)$$

[In the absence of final-state interactions, α_i is zero and Eq. (1) gives the step-function one-electron threshold law.]

Attempts to compare quantitatively the predicted threshold law with experimental data have been frustrated by the absence of accurate values of the parameters A_i and ξ , and by uncertainties about the precise values of the phase shifts and the form of the net electron-hole interaction. Nevertheless, two qualitative predictions³ of the many-electron theory seem to have been confirmed by observations: (1) For forbidden transitions from s-like core levels to even-parity conduction bands, A_0 is zero and the p-wave exponent α_1 is often negative: The electron-hole interaction causes a suppressed, rounded threshold shape. (2) For allowed transitions, A_0 is non-zero, the s-wave exponent α_0 is normally positive, and $\epsilon_2(\omega)$ exhibits a divergent "spike anomaly."

The purposes of this paper are (1) to emphasize that the Friedel sum rule relates the exponents α_0 and α_1 , (2) to derive a set of inequalities